Available online at www.sciencedirect.com
ScienceDirect
Ceramics International 35 (2009) 597–602
CERAMICS INTERNATIONAL
www.elsevier.com/locate/ceramint

Fabrication and characterization of cordierite-bonded porous SiC ceramics

Shifeng Liu [a,b], Yu-Ping Zeng [a,*], Dongliang Jiang [a]

[a] Shanghai Institute of Ceramics, Chinese Academy of Science, 1295 Dingxi Road, Shanghai 200050, China
[b] Graduate School of the Chinese Academy of Science, Beijing 100039, China

Received 10 September 2007; received in revised form 14 November 2007; accepted 14 January 2008
Available online 24 April 2008

Abstract

A reaction bonding technique was used for the preparation of cordierite-bonded porous SiC ceramics in air from α-SiC, α-Al_2O_3 and MgO, using graphite as the pore-forming agent. Graphite was burned out to produce pores and the surface of SiC was oxidized to SiO_2 at high temperature. With further increasing the temperature, SiO_2 reacted with α-Al_2O_3 and MgO to form cordierite. SiC particles were bonded by the cordierite and oxidation-derived SiO_2. The reaction bonding characteristics, phase composition, open porosity, pore size distribution and mechanical strength as well as microstructure of porous SiC ceramics were investigated. The pore size and porosity were strongly dependent, respectively, on graphite particle size and volume fraction. The porous SiC ceramics sintered at 1350 °C for 2 h exhibited excellent combination properties, the flexural strength of 26.0 MPa was achieved at an open porosity of 44.51%.

Keywords: D. Cordierite; D. SiC; Porous ceramics; Reaction bonding

1. Introduction

Recently, porous SiC ceramics have been a focus of research in the field of porous ceramics due to their high strength and excellent mechanical and chemical stability. Porous SiC ceramics have been considered as one of the most ideal candidates for hot-gas or molten-metal filters, gas-burner media, catalytic supports, thermal insulators and refractory materials [1–7]. However, a high temperature about 2100 °C is needed for the pressureless sintering of SiC ceramics because of the strong covalent nature of Si–C bond, which limits the practical applications of porous SiC ceramics [8]. Much work had been done to lower the processing temperature of porous SiC ceramics. She et al. [9,10] have developed an oxidation-bonding technique for the fabrication of porous SiC ceramics at low temperature, SiC particles were bonded by the oxidation-derived SiO_2 glass and the oxidation bonded porous SiC (OBSC) ceramics exhibit high flexural strength and excellent oxidation resistance. Furthermore, with Al_2O_3 addition, mullite-bonded porous SiC ceramics with good thermal shock resistance and better high temperature stability and oxidation resistance were prepared [11,12].

It is well known that cordierite ($2MgO{\cdot}2Al_2O_3{\cdot}5SiO_2$) has a low coefficient of thermal expansion [13], in addition, cordierite can be synthesized at low temperature [14,15], so, cordierite is chosen as the bonding phase to fabricate porous SiC ceramics in the present work. The objective of this work is to fabricate cordierite-bonded porous SiC ceramics from α-SiC, α-Al_2O_3 and MgO in air by the reaction bonding process at relatively low temperatures, using graphite powder as the pore-forming agent. The reaction bonding characteristics, phase composition, porosity, pore size distribution, mechanical strength and microstructure of porous SiC ceramics were investigated as a function of sintering conditions and Al_2O_3 + MgO additions as well as graphite particle size and content.

2. Experimental procedure

Commercially available α-SiC powder (99.4% purity, 10.0 μm, Weifang Kaihua Silicon Carbide Micro-powder Co. Ltd., Weifang, China) α-Al_2O_3 (99.9% purity, 0.6 μm,

* Corresponding author. Tel.: +86 21 52415203; fax: +86 21 52413903.
E-mail address: yuping-zeng@mail.sic.ac.cn (Y.-P. Zeng).

0272-8842/$34.00
doi:10.1016/j.ceramint.2008.01.025

Wusong, Chemical Fertilizer Factory, Shanghai, China) and MgO (>98% purity, Shanghai Tongya Chemical Technology Co. Ltd., Shanghai, China) were used as the starting materials. Three types of graphite powders (99.9% purity, Qingdao Huatai Lubricant Sealing Science and Technology Co. Ltd., Qingdao, China) with an average particle size of 5.0, 10.0 and 20.0 μm were employed, respectively, as the pore-forming agents.

The powder mixtures of SiC, Al_2O_3·MgO and C as listed in Table 1 were ball-milled in ethanol for 24 h to obtain homogeneous slurries, where we defined the weight fractions of Al_2O_3 + MgO in SiC + Al_2O_3 + MgO as x and the volume fraction of C in SiC + Al_2O_3 + MgO + C as y, the weight ratio of Al_2O_3 to MgO was fixed to the value of 2.53, which is equal to the ratio of Al_2O_3 to MgO in the stoichiometric composition of cordierite, adding proper quantities PVB (Polyvinyl Butyral) as binder. After being dried in a dry oven at 80 °C and sieved through a 75-mesh screen, the mixed powders were bidirectionally pressed into the rectangular specimens with dimensions of ~5.0 mm × 10.0 mm × 50.0 mm under a 56 MPa pressure using a steel die. The specimens were sintered in air at 1200–1400 °C for different soaking time with a heating and cooling rate of 5 °C/min.

All specimens were weighted before and after sintering to calculate the oxidation degree of SiC particles. Oxidation behavior and phase transformation characteristics of composition were evaluated, respectively, by thermogravimetry (TG) and thermal difference analysis (DTA) (Model STA 449C, Netzsch Co. Ltd., Germany) in air at a heating rate of 5 °C/min until 1400 °C. Open porosity and bulk density were determined by the Achimedes method with distilled water as the liquid medium. Pore size distribution was characterized by the mercury porosimetry (Model Pore-Sizer 9320, Micromeritics, USA). Phase analysis was conducted by X-ray diffraction (XRD) (Model RAX-10, Rigacu, Japan) with Cu Kα radiation. Microstructures were observed by scanning electron microscopy (SEM) (Model JSM-5600LV, JEOL, Japan). Flexural strength was measured via the three-point bending test (Model AUTOGRAPH AG-1, Shimadzu, Japan) with a support distance of 30 mm and a cross-head speed of 0.5 mm/min, four specimens were tested to obtain the average strength and standard deviation.

Table 1
Compositions of the powder mixtures for porous SiC ceramics synthesis, where x and y were the weight fractions of Al_2O_3 + MgO in SiC + Al_2O_3 + MgO and the volume fraction of C in SiC + Al_2O_3 + MgO + C, respectively

Mixture	$x\left(\frac{Al_2O_3+MgO}{SiC+Al_2O_3+MgO}\right)$	$y\left(\frac{C}{SiC+Al_2O_3+MgO+C}\right)$	Average particle size of graphite (μm)
1	0.10	0.25	10.0
2	0.15	0.25	10.0
3	0.20	0.25	10.0
4	0.30	0.25	10.0
5	0.20	0	–
6	0.20	0.40	10.0
7	0.20	0.50	10.0
8	0.20	0.60	10.0
9	0.20	0.25	5.0
10	0.20	0.25	20.0

3. Results and discussion

3.1. Reaction bonding behavior

Fig. 1 shows the TG-DTA curves of the green compact of mixture 3. As can be seen from the TG curve, there is an obvious weight loss from ~600 to ~890 °C, and a slow weight gain from ~900 to ~1200 °C, but a rapid weight gain from ~1200 to ~1400 °C. It is known C oxidation begins at ~600 °C and completes at ~900 °C, while SiC starts to oxidize to SiO_2 at ~750 °C [12]. So it can be inferred that SiC oxidized slowly from ~750 to ~1200 °C while rapidly from ~1200 to ~1400 °C in the present work. Fig. 2 shows the plot of SiC oxidation degree versus sintering temperature during the fabrication of porous SiC ceramics with mixture 3 as starting materials. As can be seen, the oxidation degree of SiC increases from 13.09% to 45.63% with elevating the sintering temperature from 1200 to 1400 °C, this result is consistent with the former analysis to TG curve very well. It is shown in the DTA curve that there are three exothermal peaks, respectively, near 1255.4, 1292.3 and 1346.7 °C, while an endothermic peak near 1327.3 °C. The peak near 1255.4 °C is attributed to the formation of α-cordierite, which can be confirmed by the investigation to the phase compositions of samples sintered at different temperatures. As shown in Fig. 3, SiC, cristobalite and spinel peaks exist at all the five sintering temperatures, weak α-cordierite peaks appear at 1250 °C, while no other new phase has formed upon 1250 °C. In addition, the peak intensity of α-cordierite is found to rise continuously as temperature increases from 1250 to 1350 °C, while the peak intensity of spinel has not obviously change as temperature increases, so it can be inferred that the other two exothermal peaks near 1292.3 and 1346.7 °C are also corresponding to the formation of α-cordierite, and the endothermic peak near 1327.3 °C results from the formation of Mg–Al–Si–O glass phase. According to the work by Shi et al. [14], the dissolution of MgO and Al_2O_3 into SiO_2 results at the initial stage where α-cordierite forms, the solid solution starts to turn into α-cordierite at its limit of solubility, so, in the present work, the exothermal peak near 1255.4 °C may be attributed to the solid solution turning into α-cordierite, its onset temperature is ~1246.5 °C.

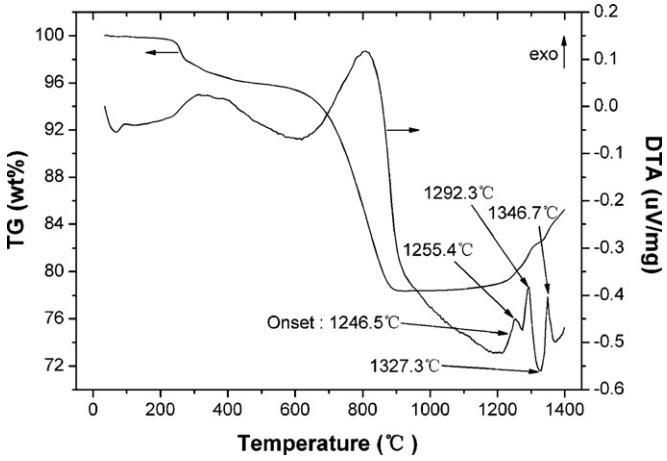

Fig. 1. TG-DTA curves of green compact of mixture 3.

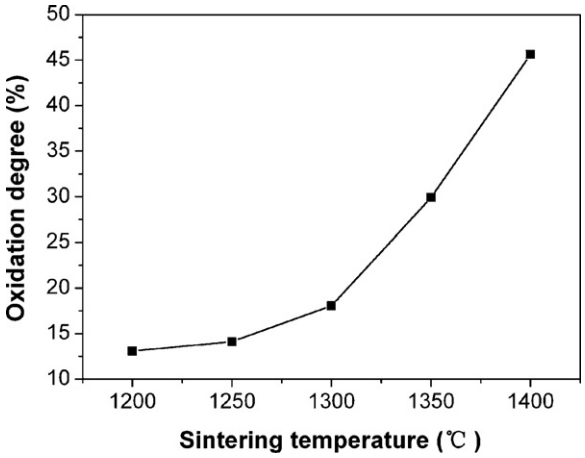

Fig. 2. Plot of oxidation degree of SiC vs. sintering temperature for the samples with $x = 0.20$ and $y = 0.25$ sintered at indicated temperature for 2 h in air, where the 10.0 μm graphite was used as the pore-forming agent.

The exothermal peak near 1292.3 °C is put down to the solid-state reaction to form α-cordierite as a result of spinel and cristobalite interaction [15–17]; while the last exothermal peak near 1346.7 °C corresponds to crystallizing α-cordierite from Mg–Al–Si–O glass. Thus, the sintering of porous SiC ceramics is realized by a series of reactions as follows:

$$SiC + 2O_2 \rightarrow SiO_2 + CO_2 \quad (1)$$

$$MgO + Al_2O_3 \rightarrow MgO \cdot Al_2O_3\ (\text{spinel}) \quad (2)$$

$$2MgO + 2Al_2O_3 + 5SiO_2 \rightarrow 2MgO \cdot 2Al_2O_3 \cdot 5SiO_2\ (\text{cordierite}) \quad (3)$$

$$2MgO \cdot Al_2O_3 + 5SiO_2 \rightarrow 2MgO \cdot 2Al_2O_3 \cdot 5SiO_2 \quad (4)$$

Based on above analyses, porous SiC ceramics with cordierite as the main bonding phase can be fabricated at 1300–1400 °C. To determine suitable sintering conditions, a preliminary investigation was conducted on the powder compacts of mixture 3. Since strength and porosity are two important parameters to be considered for the applications of porous SiC ceramics, they were evaluated as a function of sintering temperature and soaking time. It can be seen from Fig. 4, the flexural strength increases slightly with temperature increasing from 1200 to 1300 °C, but increase significantly with temperature increasing from 1300 to 1350 °C, while the open porosity decreases continuously with temperature increasing from 1200 to 1350 °C. In addition, the flexural strength and the open porosity both decrease as the temperature is further increased to 1400 °C. An increase in flexural strength was achieved by extending the soaking time from 1 to 2 h at 1350 °C, while a decrease was observed as the soaking time was further extended to 4 h. So, the sintering temperature was fixed at 1350 °C and the soaking time was fixed to 2 h in the following experiments.

3.2. Microstructural characteristics

Fig. 5 shows the typical microstructure of the as-fabricated cordierite-bonded porous SiC ceramics sintered at 1350 °C for 2 h. Clearly, the connected-pores and the well-developed necks are formed between SiC particles. The pores are mainly derived

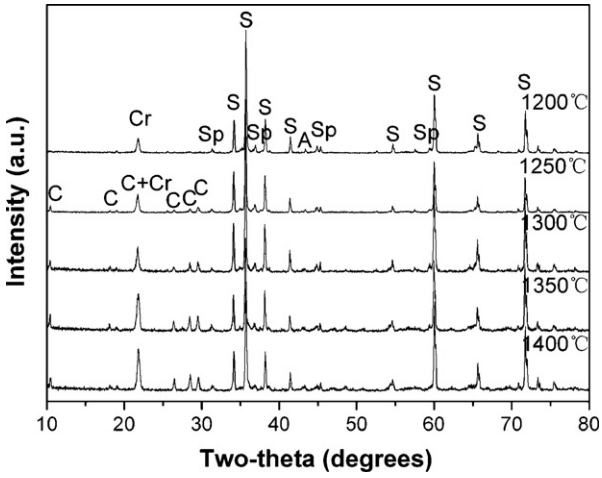

Fig. 3. XRD patterns of the specimens with $x = 0.20$ and $y = 0.25$ sintered at indicated temperature for 2 h in air, where the 10.0 μm graphite was used as the pore-forming agent. (S is SiC, Cr is cristobalite, A is α-Al_2O_3, Sp is spinel and C is α-cordierite).

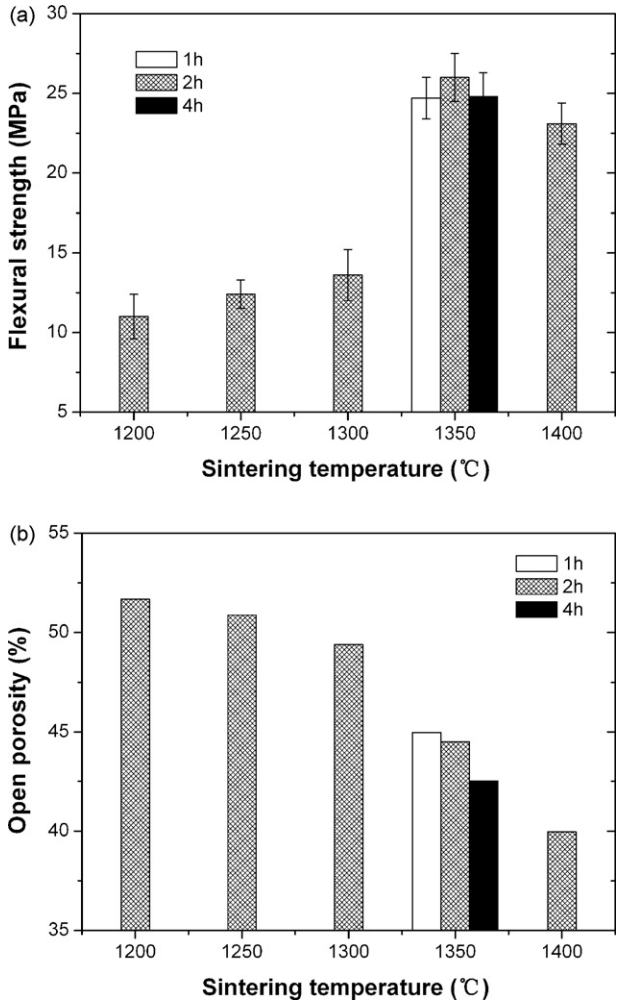

Fig. 4. (a) Flexural strength and (b) open porosity as a function of sintering temperature and soaking time for a powder compact with $x = 0.20$ and $y = 0.25$, where the 10.0 μm graphite was used as the pore-forming agent.

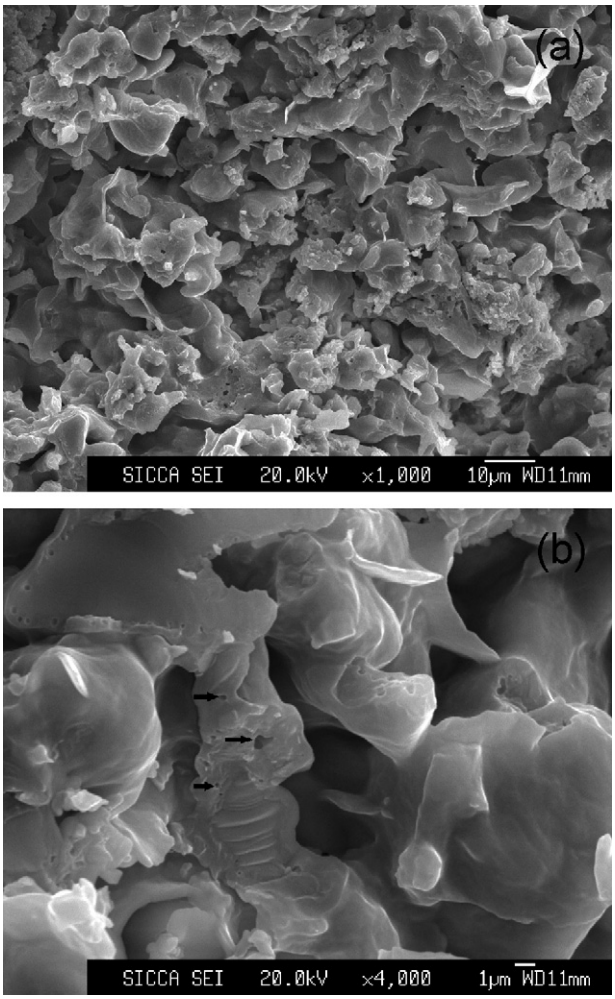

Fig. 5. SEM micrograph of fracture surfaces of cordierite-bonded porous SiC ceramics specimens with $x = 0.20$ and $y = 0.25$, where the 10.0 μm graphite was used as the pore-forming agent.

from burning out graphite and stacking SiC particles. Since 10.0 μm SiC and 10.0 μm graphite are used, the pores originating from the stacking of SiC particles are smaller than those originating from the burning out of graphite. In addition, there are many smaller closed pores in the necks as shown in Fig. 5(b) marked by arrows, and they may be caused by the retained gas in glass phase formed in sintering, but there are not enough experimental results to support this explanation, and further work should be done to explain this phenomenon.

3.3. Effects of Al_2O_3 + MgO additions on the phase compositions and properties of the porous SiC ceramics

Fig. 6 shows the XRD patterns of porous SiC ceramics specimens with different amounts of Al_2O_3 + MgO additions. As can be seen, the cordierite peak intensity increases notably with the weight fraction of Al_2O_3 + MgO in SiC + Al_2O_3 + MgO system increasing from 0.10 to 0.20, while there is only a slight increase when the weight fraction of Al_2O_3 + MgO in SiC + Al_2O_3 + MgO goes from 0.20 to 0.30. In addition, the amount of spinel increases continuously with

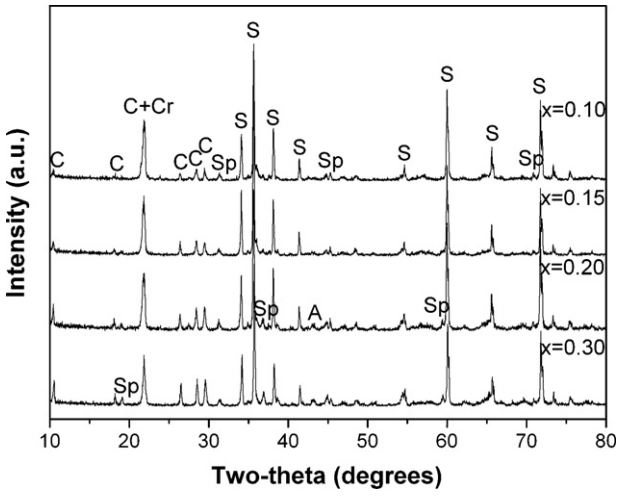

Fig. 6. XRD patterns of the specimens with different Al_2O_3 + MgO additions sintered at 1350 °C for 2 h in air, where the 10.0 μm graphite was used as the pore-forming agent and the volume fraction of C in SiC + Al_2O_3 + MgO + C was 0.25. (S is SiC, Cr is cristobalite, A is α-Al_2O_3, Sp is spinel and C is α-cordierite).

the amount of Al_2O_3 + MgO additions, as demonstrated in Fig. 6 by the strengthened intensity of the spinel peaks.

The oxidation degree, open porosity and flexural strength of the porous SiC ceramics specimens with different Al_2O_3 + MgO additions are summarized in Table 2. When the weight fraction of Al_2O_3 + MgO in SiC + Al_2O_3 + MgO increases from 0.10 to 0.30, the oxidation degree of SiC increases slightly from 28.88% to 30.98% and the open porosity decreases from 48.42% to 42.51%. However, the flexural strength first increases significantly and reaches the highest value of 26.0 MPa at $x = 0.20$, and then decreases slightly attributed to the fact that the increase of Al_2O_3 + MgO additions results in more cordierite, spinel and Mg–Al–Si–O glass. Cordierite and spinel can enhance the strength of porous SiC ceramics, but the strength is impaired when excessive Mg–Al–Si–O glass exists in the porous ceramics because this glass is fragile. As a result, too much Al_2O_3 + MgO additions are adverse to the strength of porous SiC ceramics.

3.4. Effects of graphite contents on the properties of the porous SiC ceramics

Table 3 lists the oxidation degree, open porosity and flexural strength of the porous SiC ceramics specimens with different

Table 2
Effects of Al_2O_3 + MgO additions on oxidation degree, open porosity and flexural strength for the porous SiC ceramics specimens with $y = 0.25$, where the 10.0 μm graphite was used as the pore-forming agent

x	Oxidation degree (%)	Open porosity (%)	Flexural strength (MPa)
0.10	28.88	48.42	13.9 ± 0.4
0.15	29.30	45.92	17.8 ± 1.2
0.20	29.90	44.51	26.0 ± 1.5
0.30	30.98	42.51	23.5 ± 3.0

Table 3
Effects of graphite content on the oxidation degree, open porosity and flexural strength for the porous SiC ceramics specimens with $x = 0.20$, where the 10.0 μm graphite was used as the pore-forming agent

y	Oxidation degree (%)	Open porosity (%)	Flexural strength (MPa)
0	23.09	28.07	70.3 ± 2.8
0.25	29.90	44.51	26.0 ± 1.5
0.40	37.90	54.16	9.9 ± 1.9
0.50	44.18	61.31	5.4 ± 1.1
0.60	48.98	65.69	2.9 ± 0.9

graphite loadings. With graphite loading increasing, oxidation degree and open porosity both increase significantly, while flexural strength decreases sharply. As listed in Table 3, the flexural strength decreases from 70.3 to 2.9 MPa when the volume fraction of C in SiC + Al_2O_3 + MgO + C increases from 0 to 0.60.

According to the work by Rice [18,19], the strength-porosity dependence can be approximated as follows:

$$\sigma = \sigma_0 \exp(-bp) \quad (5)$$

where σ is the strength of the porous structure at a porosity p, σ_0 is the strength of a nonporous structure, and b is an empirical constant that is dependent on the pore characteristics. From the literature [10], the closed porosity of SiC ceramics was about 0.3–0.4% when the 2.3 μm SiC powders were used. Another work [20] has shown that every inclusion is connected to the same percolating network at a volume of ≥22%. In the present work, the volume fraction of pores in all green compacts was >35%. Thus, all the pores in the compacts should be connected with each other, giving rise to an open porous network. As a result, the closed porosity of porous SiC ceramics in the present work can be neglected. Based on above analyses, the plot of flexural strength versus porosity was constructed as shown in Fig. 7. The fit of Eq. (5) to the results in Fig. 7 gave $\sigma_0 = 501$ MPa and $b = 6.97$, with a correlation factor $R^2 = 0.993$. As the R^2 value is not very high, it can be seen from Fig. 7 that the values of experimental flexural strength are lower than those of the fitting curve when porosity is high, which can be explained by the bonding phase compositions of porous SiC ceramics where different amount of graphite was added. As shown in Table 3, the oxidation degree of SiC increases from 29.90% to 48.98% with elevating the graphite content from 0.25 to 0.60, because the effectiveness of cristobalite as the bonding phase is weaker than that of cordierite, the strength-porosity dependence deviates from Eq. (5), and the values of experimental flexural strength are lower than those of the fitting curve when porosity is high.

3.5. Effects of graphite particle size on the properties of the porous SiC ceramics

The effects of graphite particle size on the oxidation degree, open porosity and flexural strength of the porous SiC ceramics specimens are listed in Table 4. As can be seen, the

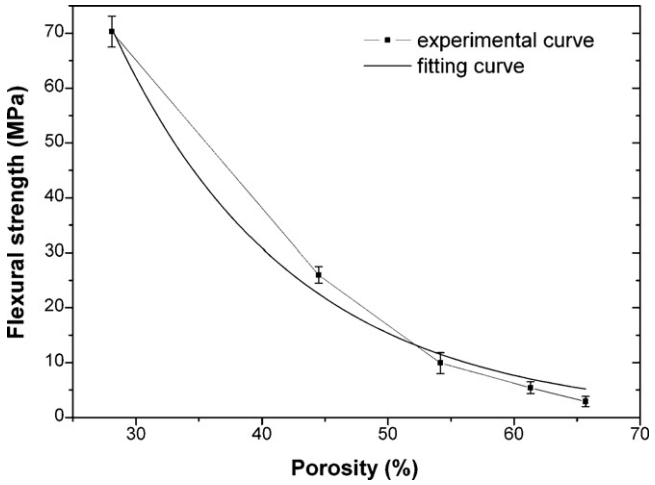

Fig. 7. Flexural strength as a function of porosity for the porous SiC ceramics with $x = 0.20$, where the 10.0 μm graphite was used as the pore-forming agent.

oxidation degree and flexural strength both decreases but the open porosity increases with the increase in graphite particle size. The degradation of the flexural strength may be caused by the increase in pore size. Further characterization of the pore size distribution in the porous SiC ceramics affirmed this inference.

Fig. 8 shows the effect of graphite particle size on the pore size distribution of porous SiC ceramics. As can be seen, the

Table 4
Effects of graphite particle size on the oxidation degree, open porosity and flexural strength for the porous SiC ceramics specimens with $x = 0.20$ and $y = 0.25$

Graphite particle size (μm)	Oxidation degree (%)	Open porosity (%)	Flexural strength (MPa)
5.0	30.28	43.88	27.1 ± 0.9
10.0	29.90	44.51	26.0 ± 1.5
20.0	26.74	44.93	25.0 ± 1.4

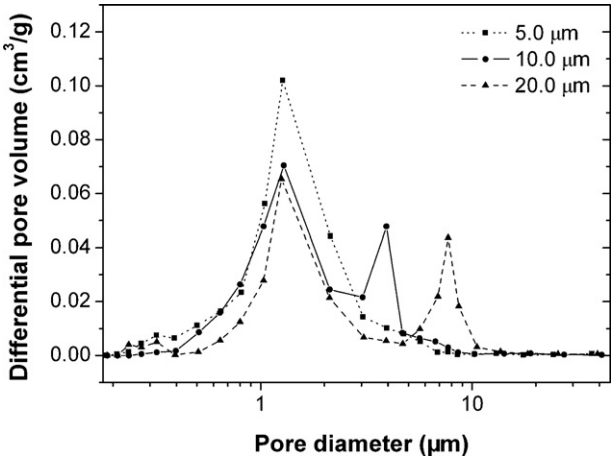

Fig. 8. Pore size distribution of the porous SiC ceramics prepared by using 5.0, 10.0 and 20.0 μm graphite particles as pore-forming agents, respectively, where $x = 0.20$ and $y = 0.25$.

pore size distribution exhibits unimodal distribution for the specimen using 5.0 μm graphite as pore-forming agent, while exhibits bimodal distribution for the specimens using 10.0 or 20.0 μm graphite as pore-forming agents. This is because the size of the pores formed by stacking SiC particles approximate to that of pores derived from burning out graphite particles when 5.0 μm graphite was used, while the graphite particle size increases to 10.0 μm or even 20.0 μm, the pores from the burnout of graphite are much larger than those from the stacking of SiC particles. It can be seen from Fig. 8 the size of the larger pores is ~7.6 μm for the specimen using 20.0 μm graphite as pore-forming agent, the value being much smaller than that of the graphite particle size, which should be attributed to the shrinkage of the pores and the fact that the pore sizes measured by mercury porosimetry are those of pore channels rather than cavities [9].

4. Conclusions

Cordierite-bonded porous SiC ceramics were fabricated in air by the reaction bonding technique from α-SiC, α-Al_2O_3 and MgO, using graphite as the pore-forming agent. The connected-pores and well-developed necks are formed between SiC particles, the pores are mainly derived from the burning out of graphite and the stacking of SiC particles. The oxidation degree of SiC increases with sintering temperature and the amount of Al_2O_3 + MgO additions as well as graphite content, but decreases with the graphite particle size. The open porosity decreases with sintering temperature and the amount of Al_2O_3 + MgO additions, but increases with graphite particle size and content. The flexural strength is in inverse proportion to the graphite particle size and content, however, the best values of the sintering temperature and the weight fraction of Al_2O_3 + MgO in SiC + Al_2O_3 + MgO are 1350 °C and 0.20, respectively. When 10.0 μm graphite was used, flexural strength of 26.0 MPa was achieved at an open porosity of 44.51%.

Acknowledgement

The authors would like to thank the ‘‘Plan of Outstanding Talents’’ of Chinese Academy of Science for the financial support.

References

[1] I. Nettleship, Applications of porous ceramics, Key Eng. Mater. 122 (1996) 305–324.
[2] P.H. Pastila, V. Helanti, A.P. Nikkila, T.A. Mantyla, Effect of crystallization on creep of clay bonded SiC filters, Ceram. Eng. Sci. Proc. 19 (1998) 37–44.
[3] M.A. Alvin, Impact of char and ash fines on porous ceramic filter life, Fuel Process. Technol. 56 (1998) 143–168.
[4] P. Pastila, V. Helanti, A.P. Nikkila, T. Mantyla, Environmental effects on microstructure and strength of SiC-based hot gas filters, J. Eur. Ceram. Soc. 21 (2001) 1261–1268.
[5] M.J. Ledoux, S. Hantzer, C.P. Huu, J. Guille, M.P. Desaneaux, New synthesis and uses of high-specific-surface SiC as a catalytic support, J. Catal. 114 (1988) 176–185.
[6] M. Benaissa, J. Werckmann, G. Ehret, E. Peschiera, J. Guille, M.J. Ledoux, Structural studies of active-carbon used in the growth of silicon-carbide catalyst support, J. Mater. Sci. 29 (1994) 4700–4707.
[7] N. Keller, C. Phan-Huu, S. Roy, M.J. Ledoux, C. Estournes, J. Guille, Influence of the preparation conditions on the synthesis of high surface area SiC for use as a heterogeneous catalyst support, J. Mater. Sci. 34 (1999) 3189–3202.
[8] L.S. Sigl, Core/rim structure of liquid-phase-sintered silicon carbide, J. Am. Ceram. Soc. 76 (1993) 773–776.
[9] J.H. She, T. Ohji, S. Kanzaki, Oxidation bonding of porous silicon carbide ceramics with synergistic performance, J. Eur. Ceram. Soc. 24 (2004) 331–334.
[10] J.H. She, J.F. Yang, N. Kondo, T. Ohji, S. Kanzaki, Z.Y. Deng, High-strength porous silicon carbide ceramics by an oxidation-bonding technique, J. Am. Ceram. Soc. 85 (2002) 2852–2854.
[11] J.H. She, T. Ohji, Z.Y. Deng, Thermal shock behavior of porous silicon carbide ceramics, J. Am. Ceram. Soc. 85 (2002) 2125–2127.
[12] J.H. She, Z.Y. Deng, J. Daniel-Doni, T. Ohji, Oxidation bonding of porous silicon carbide ceramics, J. Mater. Sci. 37 (2002) 3615–3622.
[13] M.E. Milberg, H.D. Blair, Thermal expansion of cordierite, J. Am. Ceram. Soc. 60 (1977) 372–373.
[14] Z.M. Shi, K.M. Liang, S.R. Gu, effects of CeO_2 on phase transformation towards cordierite in MgO–Al_2O_3–SiO_2 system, Mater. Lett. 51 (2001) 68–72.
[15] R. Goren, H. Gocmez, C. Ozgur, Synthesis of cordierite powder from talc, diatomite and alumina, Ceram. Int. 32 (2006) 407–409.
[16] S. Kumar, K.K. Singh, P. Ramachandrarao, Synthesis of cordierite from fly ash and its refractory properties, J. Mater. Sci. Lett. 19 (2000) 1263–1265.
[17] Y. Kobayashi, K. Sumi, E. Kato, Preparation of dense cordierite ceramics from magnesium compounds and kaolinite without additives, Ceram. Int. 26 (2000) 739–743.
[18] R.W. Rice, Comparison of stress concentration versus minimum solid area based mechanical property-porosity relations, J. Mater. Sci. 28 (1993) 2187–2190.
[19] R.W. Rice, Evaluation and extension of physical property-porosity models based on minimum solid area, J. Mater. Sci. 31 (1996) 102–118.
[20] F.F. Lange, L. Atteraas, F. Zok, J.R. Porter, Deformation consolidation of metal powders containing steel inclusions, Acta Metall. Mater. 39 (1991) 209–219.